Comparison between Ir, Ir 0.85 Rh 0.15 and Ir 0.7 Rh 0.3 thin films as electrodes for surface acoustic waves applications above 800°C in air atmosphere

Amine Taguett, Thierry Aubert, Omar Elmazria, Florian Bartoli, Marc Lomello, Michel Hehn, Jaafar Ghanbaja, Pascal Boulet, Stéphane Mangin, Yong Xu

HAL Id: hal-01628903
https://hal.science/hal-01628903

Submitted on 9 Nov 2017

Comparison between Ir, $Ir_{0.85}Rh_{0.15}$ and $Ir_{0.7}Rh_{0.3}$ thin films as electrodes for surface acoustic waves applications above 800°C in air atmosphere

Amine Taguett[1], Thierry Aubert[1,2], Omar Elmazria[3], Florian Bartoli[1], Marc Lomello[2], Michel Hehn[3], Jaafar Ghanbaja[3], Pascal Boulet[3], Stéphane Mangin[3], Yong Xu[3]

[1]Laboratoire Matériaux Optiques, Photonique et Systèmes (LMOPS), CentraleSupélec-Université de Lorraine, 57070 Metz, France

[2]Laboratoire SYMME, Université Savoie Mont Blanc, 74944 Annecy-le-Vieux, France

[3] Institut Jean Lamour (IJL), UMR 7198 Université de Lorraine-CNRS, 54506 Vandoeuvre-lès-Nancy, France

Abstract—In this paper, we investigate the suitability of Ir, $Ir_{0.85}Rh_{0.15}$ and $Ir_{0.7}Rh_{0.3}$ thin films as electrodes for surface acoustic waves (SAW) applications taking place above 800°C in air atmosphere. As expected, all films oxidize from 800°C in IrO_2 or $Ir_xRh_{1-x}O_2$ phase. The electrical properties of the latter remain compatible with the design of SAW devices, with a specific electrical resistance of 151 and 100 $\mu\Omega \cdot cm$ for x = 0.7 and x = 0.85 respectively. Moreover, we observe that the $Ir_xRh_{1-x}O_2$ phase is much more stable regarding sublimation effect than the IrO_2 phase, highlighting the interest of alloying Ir with Rh for high-temperature applications. SAW devices based on langasite substrate and $Ir_{0.85}Rh_{0.15}$ electrodes show a very good stability for at least several days at 800°C in air. In the case of $Ir_{0.7}Rh_{0.3}$ electrodes, this stability is extended to temperatures up to 900°C.

Keywords—**High-temperature; SAW; Ir-Rh electrodes; Multilayers film**

1. INTRODUCTION

Surface acoustic wave (SAW) sensors have a high innovation potential for use in high-temperature environments, owing to their large sensitivity to environmental conditions (temperature, pressure, strain or gas concentration), small size, and above all, the possibility to be wirelessly requested without battery or embedded electronics [1-4]. To develop such sensors, one of the main challenges to overcome is to grow highly conductive thin film electrodes, typically some hundred nanometers thick, able to withstand these harsh conditions and avoid any degradation related to agglomeration or oxidation phenomena.

In this context, various metallization structures have been previously considered and characterized. First studies were naturally made on platinum electrodes as this material shows an exceptional noble character, preventing oxidation phenomena. Moreover, the melting temperature of Pt, being equal to 1773°C, seems high enough for SAW applications taking place below 1000°C. However, 100 nm-thick Pt thin films undergo agglomeration phenomena from 700°C, resulting in a final state consisting in a collection of separate Pt beads [5]. Agglomeration phenomena are specific of thin films and are driven by atomic diffusion. Therefore, the smaller are the diffusion coefficients, the slower are agglomeration phenomena. Consequently, one relevant strategy, developed by Pereira da Cunha *et al.* consisted in using Pt-10%Rh alloys instead of pure Pt thin films, and then Pt-10%Rh/ZrO$_2$ nanocomposites. A spectacular increase in stability was observed. Thus, an LGS-based SAW device with Pt-10%Rh/ZrO$_2$ nanocomposites electrodes was operated for more than 5 months at 800°C in air atmosphere [6]. In order to reach higher temperatures, Frankel *et al.* have developed new nanocomposite films based on Pt [7]. The best performances were obtained by the Pt-Al$_2$O$_3$ and Pt-Ni/Pt-Zr compositions which show a specific electrical resistance in the order of 200 μΩ·cm after annealing in air for 4 hours in the temperature range from 1050 to 1150°C. However, the long-term stability of these films was not studied. Another relevant

work concerns Al-Ru alloys thin films [8]. The Al-Ru films were annealed between 600°C and 900°C under high vacuum conditions or under air atmosphere. The authors show that heat treatment under high vacuum conditions results in a strong reduction in the specific electrical resistance, which is in agreement with the films recrystallization observed by XRD measurements. The situation is different for the samples annealed in air. Indeed, except for the samples annealed at 600°C for which a reduction in the specific resistance was noticed as well, the samples annealed at higher temperatures are not conductive at all anymore.

Another strategy that can be employed to thwart agglomeration phenomena consists in replacing Pt by another noble metal with a higher melting point, and thus lower diffusion coefficients. In this context, iridium, whose melting point is as high as 2440°C, is an appropriate candidate. Indeed, pure Ir electrodes show a far better resistance to agglomeration phenomena than Pt electrodes under vacuum conditions [5, 9]. The use of Ir electrodes is more problematic under air atmosphere as Ir oxidizes in IrO_2 in the vicinity of 800°C. Nonetheless, IrO_2 remains yet a good electrical conductor, with a specific electrical resistance of 47 $\mu\Omega$.cm [10], i.e. only one order of magnitude above that of conventional conductors such as Al or Cu, and still significantly lower than those of some Pt-based alloys or nanocomposite thin films. A more serious issue consists in the transformation of IrO_2 into volatile IrO_3 at higher temperatures. This phenomenon occurs between 800 and 900°C [11]. However, Osamura *et al.* demonstrated that Ir-Rh alloys, used to make spark plugs with superior performance, show a far better resistance to sublimation caused by oxidation phenomena than pure Ir spark plug electrodes [12]. Consequently, Ir-Rh thin film electrodes could have a great potential for SAW applications taking place above 800°C in oxidizing atmosphere. To check this assumption, we have conducted first investigations on Ir_xRh_{1-x} thin films (x ≤ 0.5) at high temperatures [13]. This study reveals that after an annealing of four days at 800°C under air atmosphere, these films oxidize to form $Ir_xRh_{1-x}O_2$ films. However,

this phase exhibits a reasonable resistivity suitable for the targeted application, especially as the Ir rate is high ($\rho \simeq 180$ $\mu\Omega \cdot$cm for x = 0.5).

In this context, the goal of the present study is to examine the behavior of the most promising Ir-rich compositions ($0.7 \leq x \leq 1$) above 800°C in air atmosphere. In particular, we inspect carefully the interest of alloying Ir with Rh regarding the sublimation effect described hereinabove. In a second time, we investigate the reliability of SAW devices based on $Ir_{0.7}Rh_{0.3}$ or $Ir_{0.85}Rh_{0.15}$ electrodes and langasite (LGS) substrate during a 20 days-annealing period between 800 and 950°C in air.

2. EXPERIMENTAL

Pure Ir thin films, as well as $Ir_{0.85}Rh_{0.15}$ and $Ir_{0.7}Rh_{0.3}$ multilayers thin films were deposited on (0°, 140°, 25°) LGS substrates by sputtering method. LGS was chosen for this study, focusing on electrode composition, as this piezoelectric material is known for its stability under high-temperature air atmosphere [14]. Moreover, the knowledge of the high-temperature physical constants set of LGS is currently rather good, allowing the design of efficient SAW devices [15]. A 10 nm-thick tantalum adhesion layer was firstly deposited on these substrates. Concerning the multilayers films, the respective thickness of the pure Ir and Rh nanolayers alternatively sputtered was calculated in order to control the overall stoichiometry of the films. The thickness of all considered films was fixed to 120 nm. Thus, to obtain $Ir_{0.85}Rh_{0.15}$ films, three 34 nm-thick Ir films were alternatively sputtered with three 6 nm-thick Rh layers. In the case of the $Ir_{0.7}Rh_{0.3}$ films, six 14 nm-thick Ir films were alternatively sputtered with six 6 nm-thick Rh layers. The resistivity of all the as-deposited samples measured using four points method is about 14 $\mu\Omega \cdot$cm, and is independent from their composition.

Some samples then underwent three successive annealing periods at 800°C: the first one lasted for 4 days and the next ones 7 days each. Some other samples underwent a 7 days-annealing period at 900°C after the first 4 days-annealing process at 800°C. After each annealing period, the morphology, the microstructure, the chemical composition associated to the nanostructure, and the electrical properties of the thin films were investigated by scanning electron microscopy (SEM), X-ray diffraction (XRD) in Bragg-Brentano geometry, scanning transmission electron microscopy-energy dispersive X-Ray spectroscopy (STEM-EDS) and 4-points probe resistance measurements respectively.

Some other samples were processed using conventional photolithography and ion beam etching to carry out SAW delay lines with a wavelength of 24 µm. The devices underwent different annealing periods at temperatures ranging from 800 to 950°C. The more severe annealing process consisted in twenty successive 24h long annealing periods at four rising temperatures: 800°C (day 1 to 5), 850°C (day 6 to 10), 900°C (day 11 to 15) and finally 950°C (day 16 to 20). After each 1 day-annealing period, the morphology of the electrodes was observed by optical microscopy while the S_{21} frequency response of the SAW devices was measured at room temperature using a network analyzer (PNA 5230a, Agilent Technologies Inc., Santa Clara, CA) and an RF prober station (PM5 Suss-Microtech).

3. RESULTS AND DISCUSSION

3.1. Impact of annealing on $Ir_{0.7}Rh_{0.3}$ and $Ir_{0.85}Rh_{0.15}$ thin films

θ-2θ XRD patterns of the $Ir_{0.7}Rh_{0.3}$ and $Ir_{0.85}Rh_{0.15}$ multilayers thin films obtained before and after the successive annealing periods at 800°C are visible on Fig. 1. As-deposited samples are constituted by (111)-oriented nanograins as indicated by the broad peak at 2θ = 40.5°. It is clearly visible in the case of the $Ir_{0.7}Rh_{0.3}$ multilayers films that this signal is actually the sum of two close peaks, namely (111) Ir and (111) Rh reflexes. One can assume

that in the case of $Ir_{0.85}Rh_{0.15}$ multilayers thin films, the amount of Rh is so weak that the peak at 40.5° seems related to (111) Ir reflex only. After the first 4 days-annealing period at 800°C, the $Ir_{0.7}Rh_{0.3}$ and $Ir_{0.85}Rh_{0.15}$ multilayers thin films are almost completely oxidized. Indeed, the peak corresponding to (111)-oriented Ir and Rh nanograins has almost totally vanished (and slightly moved to 41°) while new peaks have appeared. The latter can be identified as either IrO_2 or RhO_2 reflexes. It has to be noted that this oxidation process seems slightly more intense in the case of $Ir_{0.7}Rh_{0.3}$ films than for $Ir_{0.85}Rh_{0.15}$ ones. Thus, whereas the metallic phase has totally disappeared after 11 days at 800°C in the case of the $Ir_{0.7}Rh_{0.3}$ films, a weak peak corresponding to this phase subsists even after 18 days at this temperature in the $Ir_{0.85}Rh_{0.15}$ spectrum. This difference is currently unexplained.

Some additional information about the nanostructure of the oxidized films can be deducted from the TEM cross-section images (Fig. 2) and the associated X-mapping measurements (Fig. 3) obtained after the first 4 days-annealing period at 800°C. One can observe that the initial multilayers structure was completely lost during the annealing process. Instead, the new nanostructure is constituted by large grains whose typical length is 100 nm or more, overlooked by a very thin surface layer. Based on EDS measurements, it seems that these large grains contain Ir, Rh and O elements at the same time. Consequently, the new peaks appearing in the XRD spectrum after annealing process cannot likely be attributed to pure IrO_2 or RhO_2 phases. This result is confirmed by XRD measurements: by using the XRD data collected during this study and the one obtained during our previous study about $Ir_{0.1}Rh_{0.9}$, $Ir_{0.3}Rh_{0.7}$ and $Ir_{0.5}Rh_{0.5}$ thin films [13], it appears that the lattice parameters of the oxidized phase follow well the Vegard law (Fig. 4). Consequently, we assume that this new phase can be identified as tetragonal $Ir_xRh_{1-x}O_2$. The very thin layer at the surface of the film is completely Ir-depleted. Quantitative EDS measurements reveal the Rh_2O_3 nature of this layer. Such Rh_2O_3 surface layer was also observed on the annealed $Ir_{0.5}Rh_{0.5}$ samples [13]. Its

thickness seems to depend on the initial composition of the films: the larger the Rh initial rate, the thicker the Rh_2O_3 surface layer. Indeed, this thickness was 30 nm in the case of the $Ir_{0.5}Rh_{0.5}$ films, whereas it is about 15 nm and 5 nm for the $Ir_{0.7}Rh_{0.3}$ and $Ir_{0.85}Rh_{0.15}$ samples respectively.
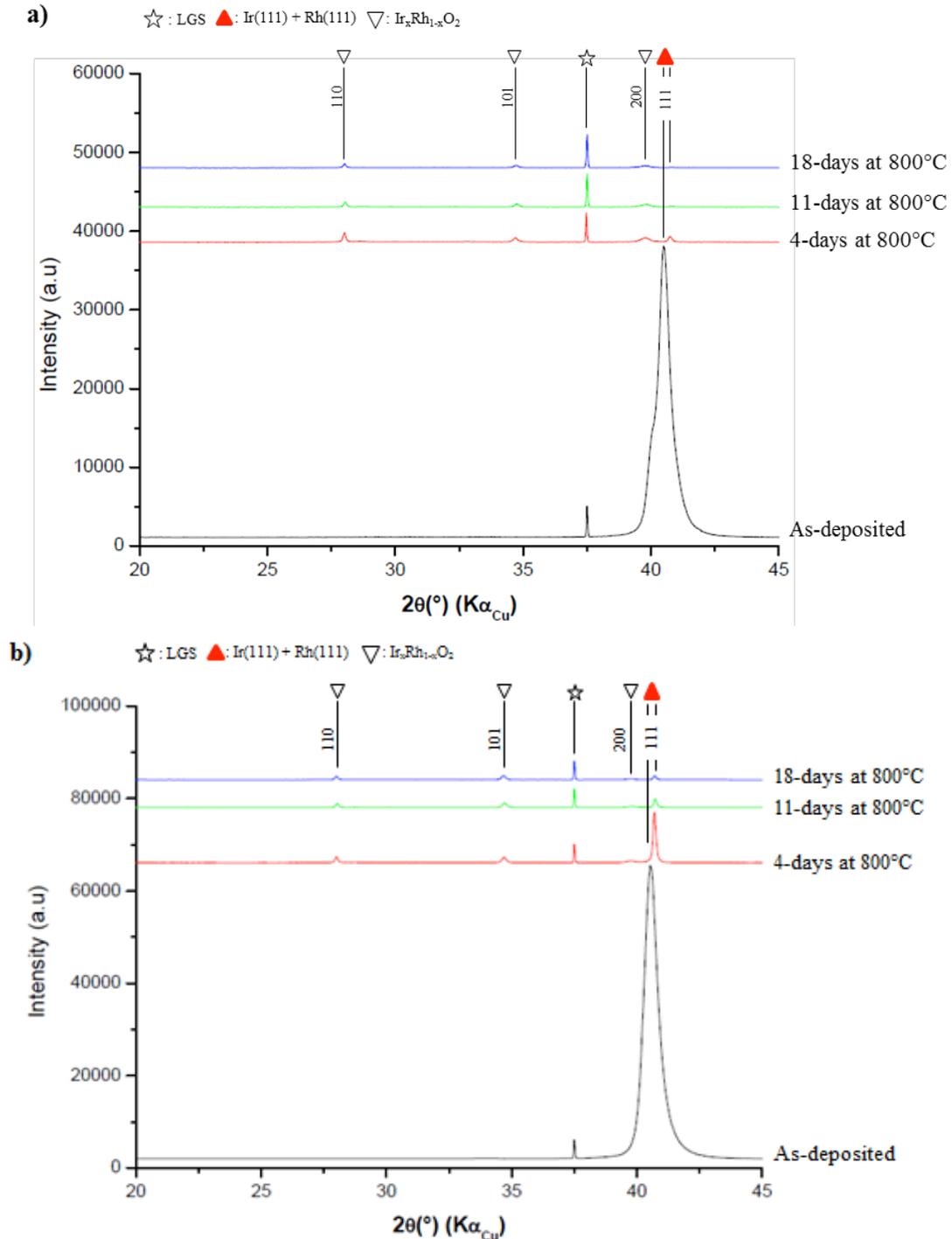

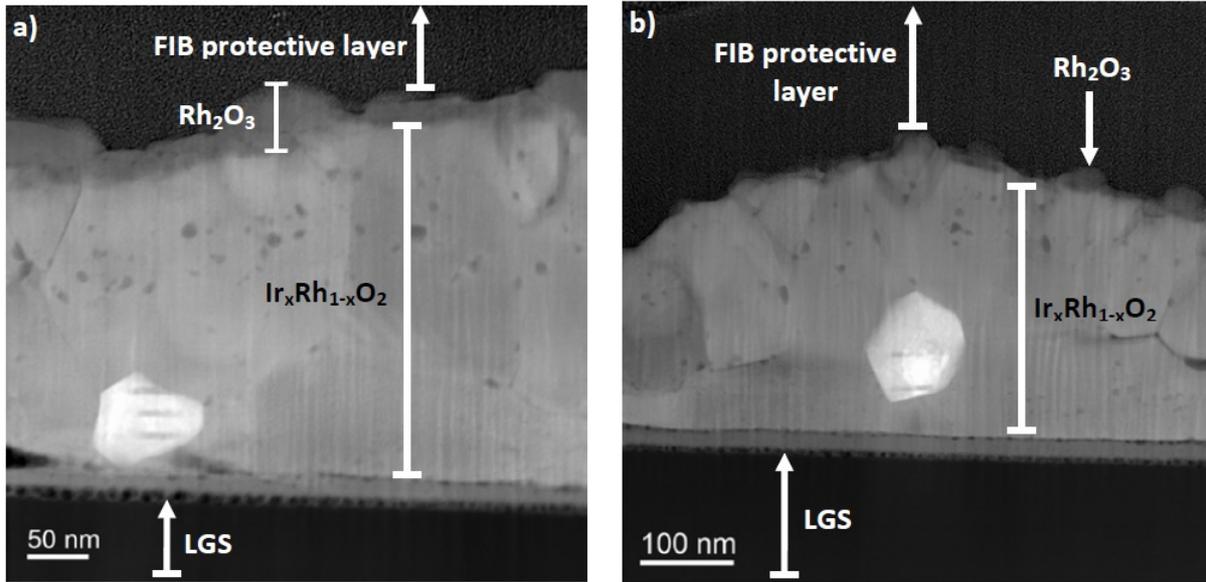Fig. 1: XRD patterns of as-deposited and annealed $Ir_{0.7}Rh_{0.3}$ (a) and $Ir_{0.85}Rh_{0.15}$ (b) films.

Fig. 2: Cross-section dark-field TEM image of the $Ir_{0.7}Rh_{0.3}$ (a) and $Ir_{0.85}Rh_{0.15}$ (b) films after a <mark>4 days-annealing</mark> period at 800°C in air.

Besides, it can be observed on both $Ir_{0.7}Rh_{0.3}$ and $Ir_{0.85}Rh_{0.15}$ films dark-field TEM images (Fig. 2) the presence of one single grain with a different shape, dimensions and contrast. In one word, this grain seems to correspond to a different phase compared to the majority of the grains. In the case of the $Ir_{0.7}Rh_{0.3}$ film, the identification of this phase is not trivial. Indeed, EDS measurements only show that both the Ir and Rh rates are slightly larger in this grain than in the neighborhood (Fig. 3a). The O rate seems the same as in the other grains. In the case of the $Ir_{0.85}Rh_{0.15}$ films, this identification is obvious. Indeed, it appears from EDS measurements that this zone is very rich in iridium, and is depleted of oxygen, especially at the heart of the grain. Thus, we assume that this grain belongs to the metallic Ir_xRh_{1-x} phase, and that the weak peak close to 41° subsisting in the $Ir_{0.85}Rh_{0.15}$ XRD spectrum comes from the presence of such metallic grains in the film. Actually, it seems that this grain is protected from oxidation by the surrounding $Ir_xRh_{1-x}O_2$ grains, which would act as a diffusion barrier. Indeed, even after 18 days at 800°C, such metallic grains still subsist as attested by the XRD spectrum of the $Ir_{0.85}Rh_{0.15}$ film. It is not currently understood why this protecting effect is more intense in the case of $Ir_{0.85}Rh_{0.15}$ than for $Ir_{0.7}Rh_{0.3}$ samples.
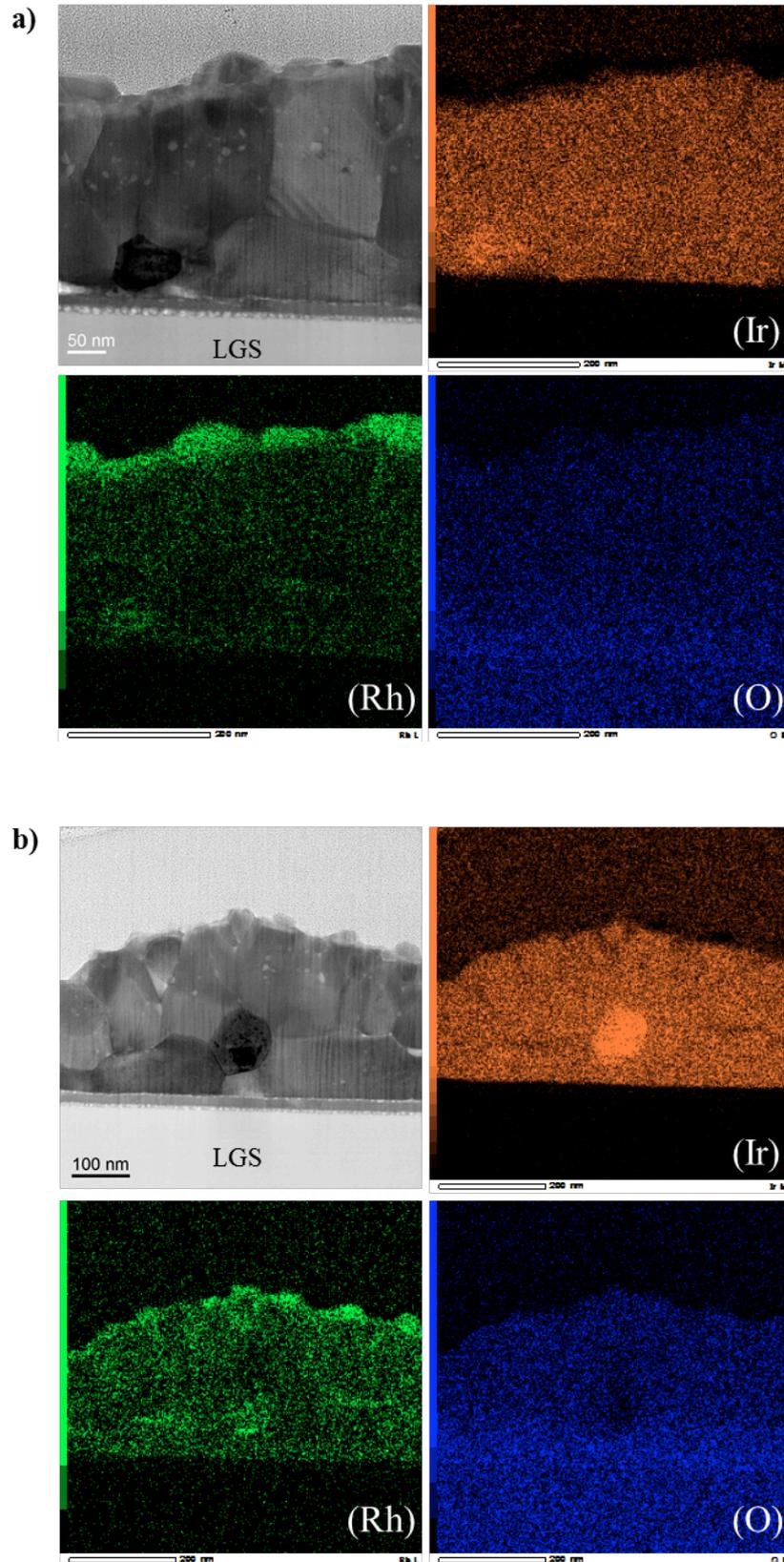
Fig. 3: **X-mapping** of the $Ir_{0.7}Rh_{0.3}$ (a) and $Ir_{0.85}Rh_{0.15}$ (b) films after a 4 days-annealing period at 800°C in air: Ir (orange), Rh (green) and O (blue).
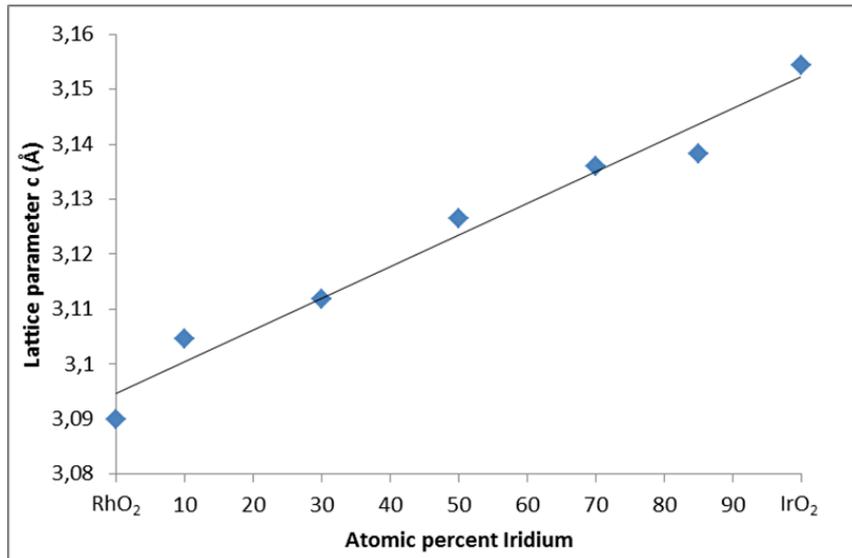
Fig. 4: Variation with composition of the c-lattice parameter of the $Ir_xRh_{1-x}O_2$ phase.

Finally, based on the determination of the post-annealing film thickness by TEM imaging and 4-points probe electrical measurements, the specific electrical resistance of the $Ir_xRh_{1-x}O_2$ phase was determined. It was found to be equal to 151 and 100 $\mu\Omega\cdot cm$ for $x = 0.7$ and $x = 0.85$ respectively. Thus, despite the oxide nature of the films, these values are very low and remain compatible with the fabrication of SAW devices. Note that this result confirms that the specific resistance of the $Ir_xRh_{1-x}O_2$ phase decreases when the Ir rate increases [13].

3.2. Interest of alloying Ir films with Rh regarding high-temperature stability

The interest of adding Rh into Ir thin films regarding sublimation effect appears at temperatures as low as 800°C if the annealing period is long enough (namely ten days or more), as shown by the electrical resistance measurements depicted in Fig. 5. After the first 4 days-annealing period at 800°C in air, the resistance of the three samples increases significantly, as the Rh content is high. Indeed, the resistance of the Ir, $Ir_{0.85}Rh_{0.15}$ and $Ir_{0.7}Rh_{0.3}$ films is approximately multiplied by 2, 3 and 4.5 respectively during this annealing

treatment, which can be attributed in the case of the $Ir_{0.85}Rh_{0.15}$ and $Ir_{0.7}Rh_{0.3}$ compositions to the oxidation process described in the previous section.

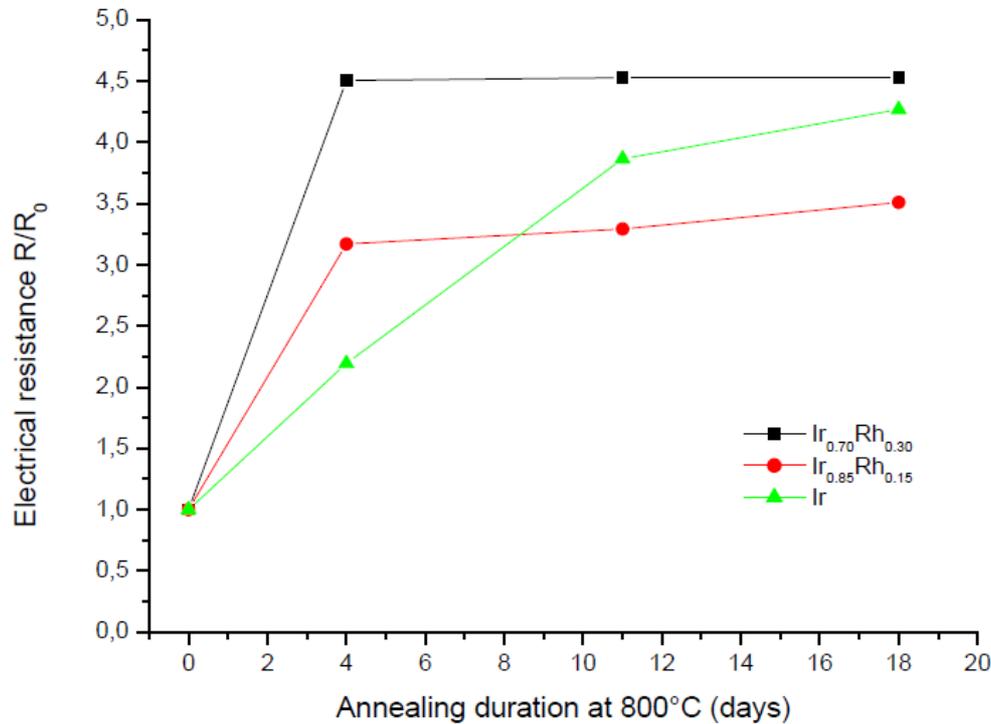**Fig. 5: Relative evolution of the electrical resistance of the Ir, $Ir_{0.85}Rh_{0.15}$ and $Ir_{0.7}Rh_{0.3}$ films during annealing at 800°C (R_0 being the resistance of the as-deposited films).**

Nevertheless, whereas the two next 7 days-annealing periods at 800°C have no effect on the $Ir_{0.7}Rh_{0.3}$ thin films and a very limited one on the $Ir_{0.85}Rh_{0.15}$ films, the electrical resistance of the sample initially consisting in pure Ir film continues increasing with time. Consequently, after 11 days at 800°C, the resistance of the $Ir_{0.85}Rh_{0.15}$ films is slightly smaller than that of Ir films. This new hierarchy is reinforced after 18 days at 800°C, while the resistance of $Ir_{0.7}Rh_{0.3}$ films is hardly larger than that of Ir films.

These phenomena can be understood thanks to θ-2θ XRD measurements carried out on the pure Ir films (Fig. 6). As-deposited films consist in (111)-oriented nanograins as shown by the large peak centered at 40.3°. Two observations can be made from the XRD spectrum obtained after the 4 days-annealing period at 800°C. Firstly, the (111) Ir peak sharpens which

is synonymous with the recrystallization of the film. However, this recrystallization process does not lead to an increase of the peak intensity. This phenomenon is related to a partial concomitant oxidation of the Ir films, as shown by the appearance of new peaks which are identified as IrO_2 reflexes. The increase in the resistance of the film observed during this annealing treatment is a consequence of this oxidation process.

At the end of the next annealing step (7 days at 800°C), the (111) Ir peak has almost totally disappeared, indicating the complete oxidation of the Ir film. However, in the same time, the intensity of the IrO_2 peaks has slightly decreased. Thus despite this steady oxidation process, the IrO_2 quantity has not increased during this annealing period. This result suggests that the transformation of the IrO_2 phase into the volatile IrO_3 already occurs at 800°C. This assumption is confirmed by the electrical measurements performed at the end of the last 7 days-annealing period. Indeed, whereas the film is already totally oxidized, the electrical resistance continues increasing, suggesting that the film thickness steadily decreases (Fig. 5).

In summary, at 800°C the Ir, $Ir_{0.85}Rh_{0.15}$ and $Ir_{0.7}Rh_{0.3}$ thin films oxidize completely (or almost completely in the case of the $Ir_{0.85}Rh_{0.15}$ samples) in a matter of days, but only the pure Ir film seems to undergo a slow destructive sublimation process. Thus, it appears that adding some Rh into Ir films leads to a significant improvement of the film resistance regarding the sublimation degradation process. The mechanism leading to this protection effect is not clear. One can just assume that the $Ir_xRh_{1-x}O_2$ phase is much more stable under oxygen than the IrO_2 phase, even if x is close to one.
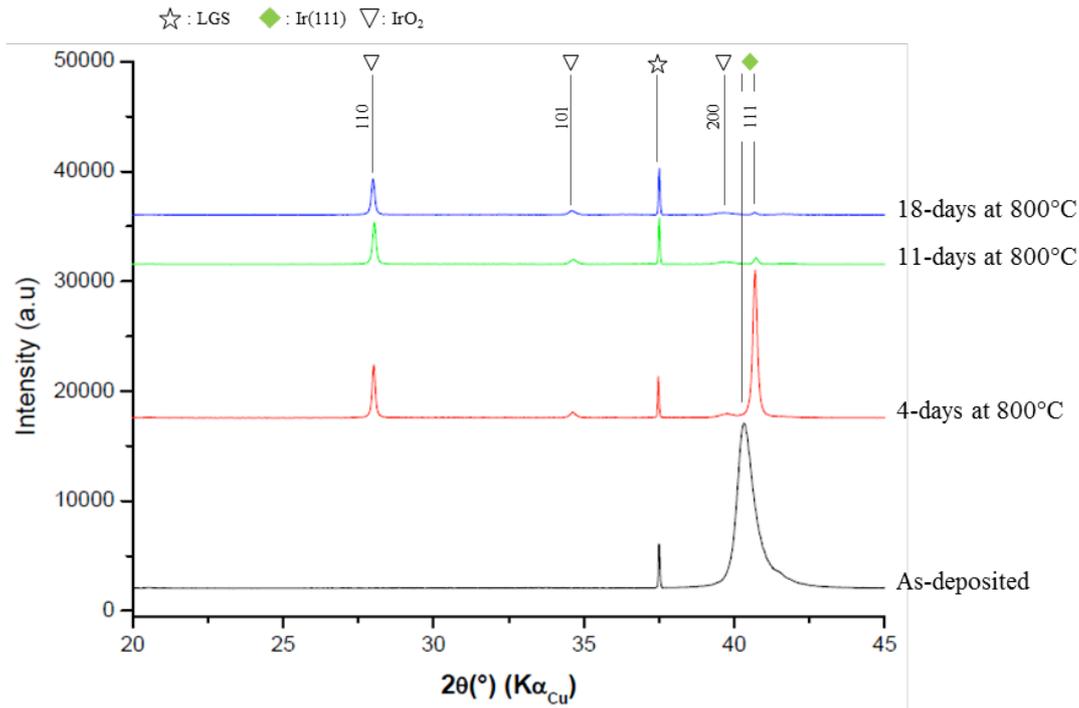
Fig. 6: As-deposited and post-annealing XRD patterns of Ir thin film.

The Rh protecting effect is even more remarkable at 900°C (Fig. 7). Indeed, the electrical resistance of the $Ir_{0.85}Rh_{0.15}$ and $Ir_{0.7}Rh_{0.3}$ samples is approximately doubled after the 7 days-annealing period at 900°C (compared to the values measured after the first 4 days-annealing period at 800°C). In the same time, Ir films are much more impacted, as the resistance gains one order of magnitude. This spectacular increase can be surely attributed to the formation of the volatile IrO_3, which occurrence is well established at 900°C, as described by several authors [11, 16]. Consequently, at the end of the annealing process (4 days at 800°C + 7 days at 900°C) the electrical resistance of Ir films is approximately three times higher than those of $Ir_{0.85}Rh_{0.15}$ and $Ir_{0.7}Rh_{0.3}$ films, both being actually very close. SEM images confirm that a surface degradation effect occurs on pure Ir films during the annealing period at 900°C, as a porous structure can be observed on these samples (Fig. 8). On the contrary, the morphology of $Ir_{0.7}Rh_{0.3}$ films seems unchanged, and that of $Ir_{0.85}Rh_{0.15}$ hardly altered.
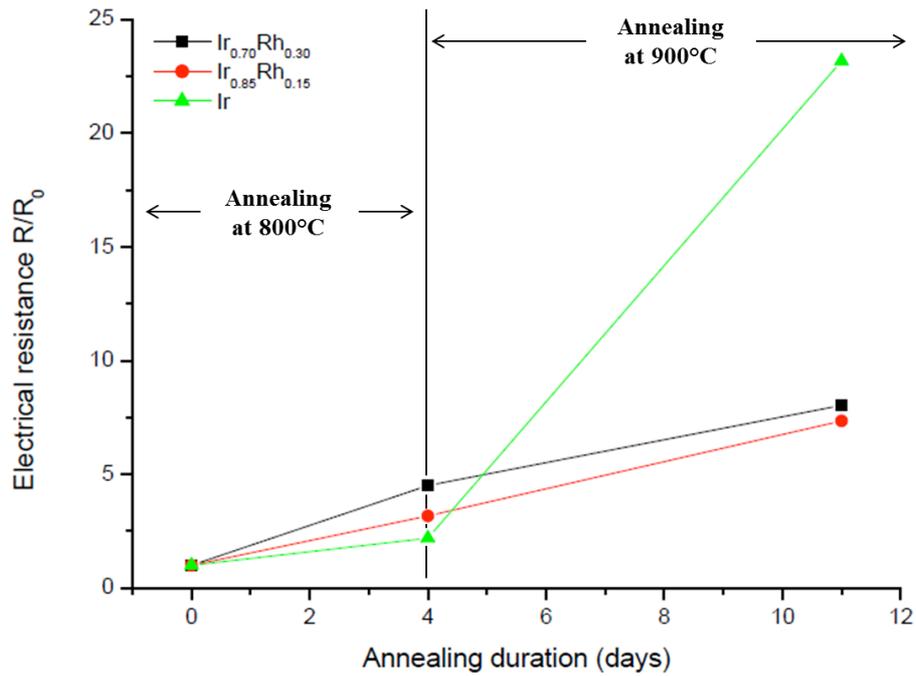
Fig. 7: Relative evolution of the electrical resistance of the Ir, Ir$_{0.85}$Rh$_{0.15}$ and Ir$_{0.7}$Rh$_{0.3}$ films during annealing process consisting of 4 days at 800°C, followed by 7 days at 900°C (R$_0$ being the resistance of the as-deposited films).
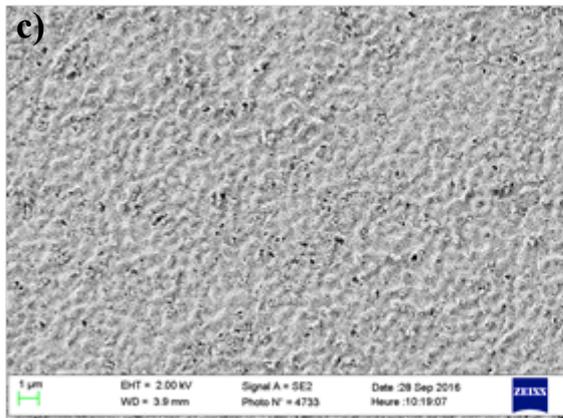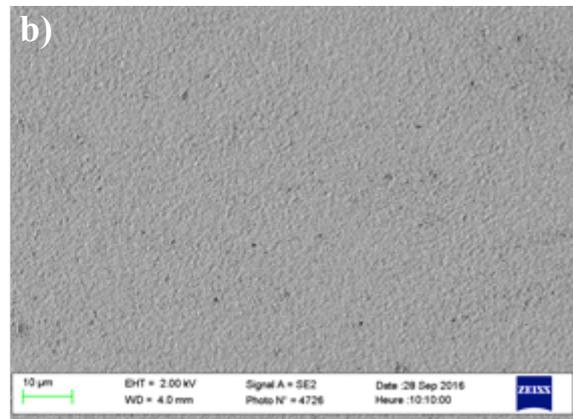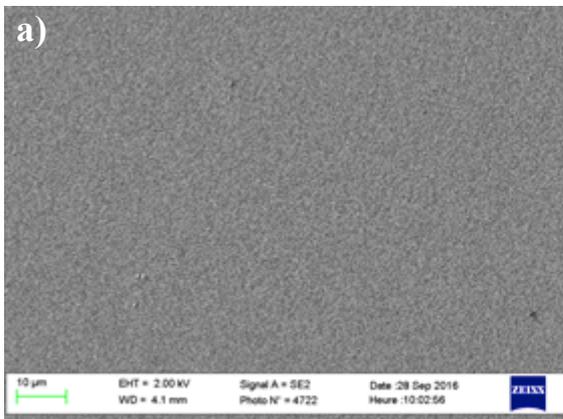

Fig. 8: SEM images showing the surface morphology after a 7 days-annealing period at 900°C in air: Ir$_{0.7}$Rh$_{0.3}$(a) Ir$_{0.85}$Rh$_{0.15}$ (b) and Ir (c) thin films.

3.3. High temperature stability tests of SAW devices

Based on the results presented in the previous sections, it appears that $Ir_{0.85}Rh_{0.15}$ and $Ir_{0.7}Rh_{0.3}$ thin films have a great potential to be used as electrodes for long-term SAW applications taking place above 800°C in air atmosphere. In order to explore this potential, SAW devices based on LGS substrate and $Ir_{0.85}Rh_{0.15}$ and $Ir_{0.7}Rh_{0.3}$ thin film electrodes were placed for a period of 4 days at 800°C and then electrically measured at room temperature. The devices were then placed in the oven for an additional period of 7 days at 800°C and measured again at the ambient. The results are presented for the devices with $Ir_{0.7}Rh_{0.3}$ thin film electrodes on Figure 9. Devices with $Ir_{0.85}Rh_{0.15}$ thin film electrodes show a similar behavior. One can observe that the insertion losses increased by 4.9 dB during the first annealing, which is certainly related to the fourfold increase in the electrical resistance value of the electrodes, as shown on Figure 5. On the contrary, no additional loss was observed during the second annealing period, and the central frequency remained mostly unchanged. This result was expected as no change in the electrode resistance was measured during this second annealing treatment (Fig. 5). This result confirms that a first annealing is required to oxidize and thus stabilize the Ir-Rh films.

In order to explore the potential of $Ir_{0.85}Rh_{0.15}$ and $Ir_{0.7}Rh_{0.3}$ thin film electrodes at higher temperatures, new samples underwent the annealing process consisting in five successive 1-day annealing periods at 800°C, then at 850°C, 900°C and finally at 950°C, as described in the experimental section. Optical microscopy shows that the electrodes morphology is not altered at all during this process (Fig. 10): no sign of agglomeration is visible.
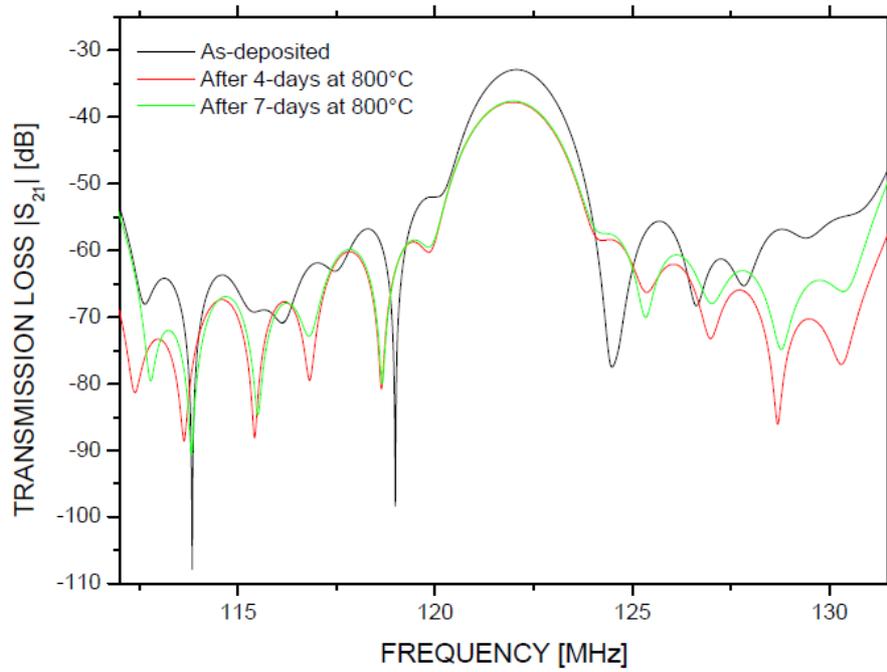
Fig. 9: Frequency response (S$_{21}$ magnitude) of a SAW delay line based on LGS substrate and 120 nm-thick Ir$_{70}$Rh$_{30}$ thin films before and after different annealing periods at 800°C in air.
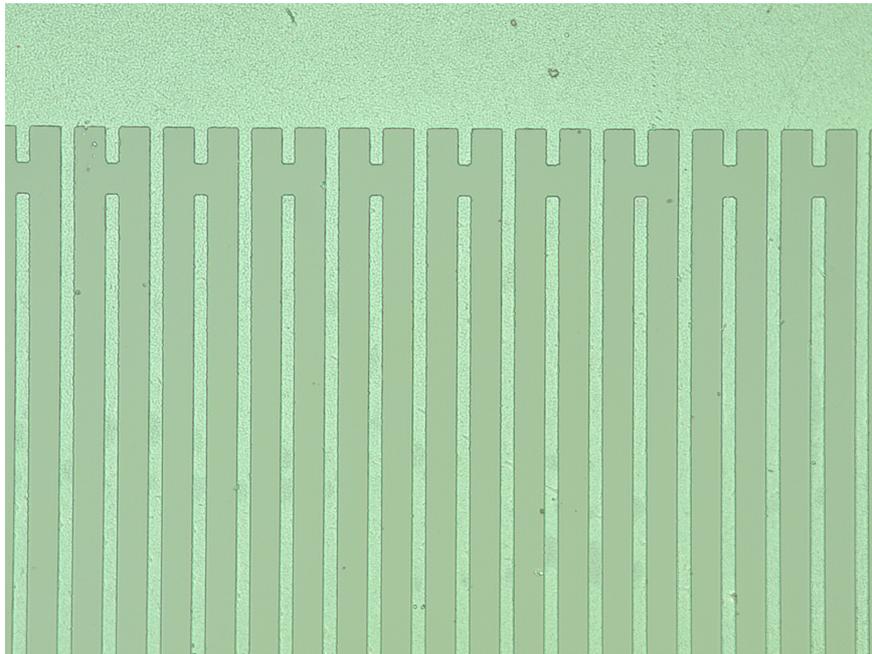

Fig. 10: Optical microscopy image of Ir$_{0.7}$Rh$_{0.3}$ electrodes taken after the fifth 1-day annealing process at 900°C

Figure 11 shows the evolution of the transmission losses of both kinds of devices all along the procedure (measurements were done at the ambient after each 1-day annealing

period). One can observe that the device based on $Ir_{0.85}Rh_{0.15}$ electrodes show an excellent stability at 800°C, but steadily degrades at 850°C, and more intensively at 900°C and 950°C. On the other side, the device based on $Ir_{0.7}Rh_{0.3}$ electrodes is very stable at 800°C and 850°C (thus the insertion losses level is exactly the same after the first annealing day at 800°C, as after 4 supplementary days at 800°C and 5 days at 850°C). The behavior is still very good at 900°C. The insertion losses increase by 2 dB after the first annealing at this temperature and then remain stable at this temperature. At 950°C, the degradation process accelerates even if after 5 days at this temperature, the signal is still clearly visible.

It has to be noticed that the stability observed at 900°C requires some ageing process at 800 and 850°C. Indeed, some other new devices underwent two successive annealing periods at 900°C, the first being twelve hours long, and the second one week long. In that case, we did not observe any signal stabilization: between the first and the second annealing periods, the insertion losses increased by 6.8 dB (Fig. 12). The mechanisms leading to the film stabilization consequently to some aging process at lower temperatures are currently not understood.
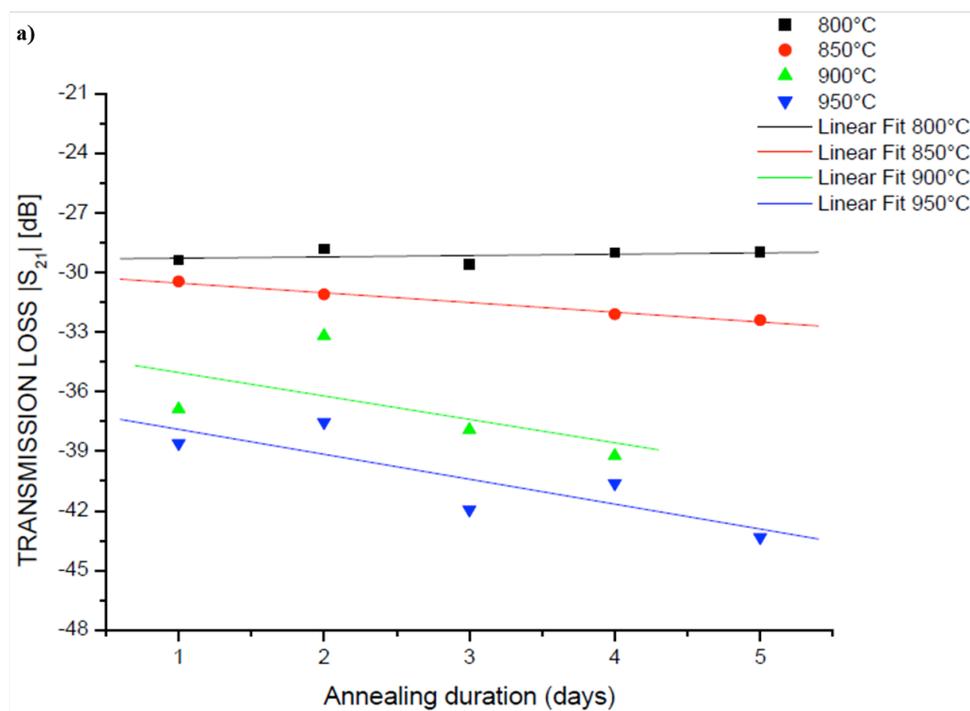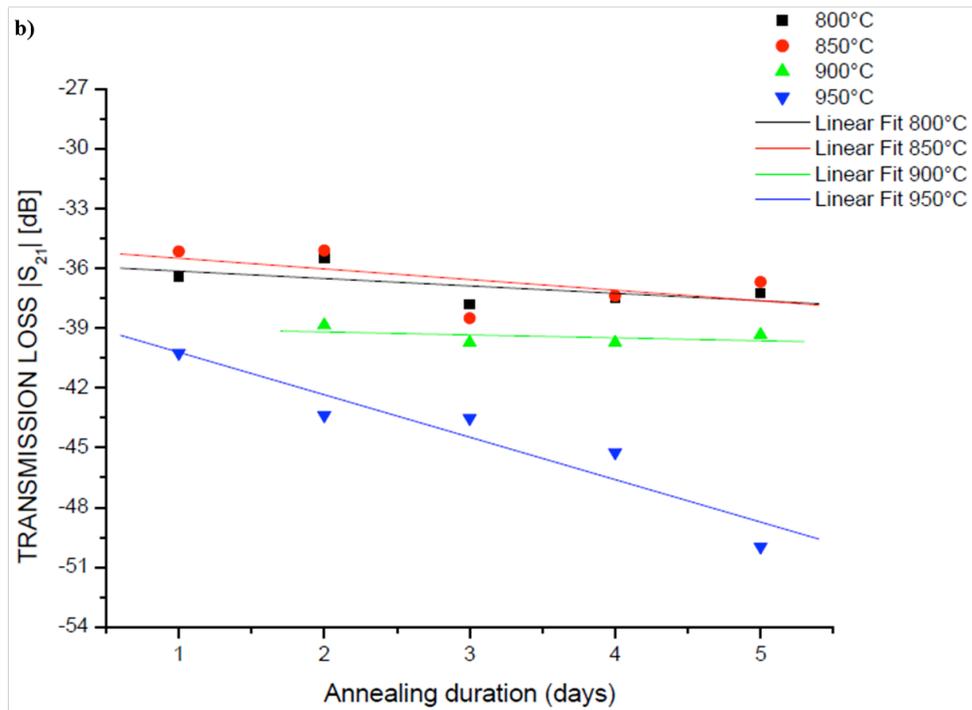
Fig. 11: Transmission losses as function of the annealing duration at different temperatures for the SAW devices based on Ir$_{0.85}$Rh$_{0.15}$ (a) and Ir$_{0.7}$Rh$_{0.3}$ (b) thin film electrodes.
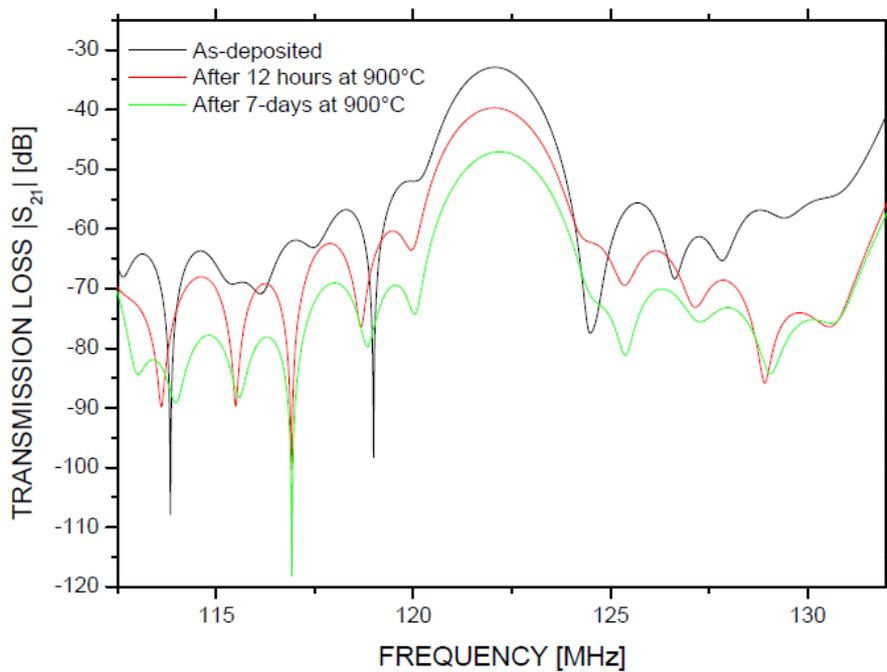

Fig. 12: Frequency response (S$_{21}$ magnitude) of a SAW delay line based on LGS substrate and 120 nm-thick Ir$_{70}$Rh$_{30}$ thin films before and after different annealing periods at 900°C in air.

4. CONCLUSION

The potential of Ir_xRh_{1-x} thin films as electrodes for SAW applications above 800°C in air has been evidenced in previous studies. This work is focused on the most promising Ir-rich compositions. Namely, 120-nm thick $Ir_{0.7}Rh_{0.3}$ and $Ir_{0.85}Rh_{0.15}$ multilayers thin films were sputtered on LGS substrates. Pure Ir thin films were also considered as reference samples. The samples underwent different annealing periods at 800 and 900°C for several days. The multilayer structure was completely lost during this heating process. Moreover, as expected, the samples oxidized to form the $Ir_xRh_{1-x}O_2$ phase. The electrical conductivity of the oxidized samples improves with the initial Ir rate. Thus, the specific electrical resistance of the $Ir_xRh_{1-x}O_2$ phase was estimated to be 151 and 100 μΩ·cm for x = 0.7 and x = 0.85 respectively, whereas it is of some tens of μΩ·cm for IrO_2. These values are all compatible with the achievement of operable SAW devices. They are also slightly lower than the ones reported for the state-of-the-art Pt-based nanocomposite films. However, as described in the literature, the most conductive IrO_2 phase sublimates into volatile IrO_3. We observed that this prohibitive phenomenon for the targeted applications already occurs at 800°C, with a slow kinetics. On the contrary, the $Ir_xRh_{1-x}O_2$ phase is much more stable, even at temperatures as high as 900°C, for several days. This result highlights the protective effect brought to Ir thin films by Rh alloying.

SAW measurements show that a first annealing cycle is necessary to oxidize and thus stabilize the Ir-based electrodes. After this stabilization process, the $Ir_xRh_{1-x}O_2$ electrodes show a great stability up to 900°C for x = 0.7 and 800°C for x = 0.85. Thus, to determine the optimal Rh rate for a given application, a trade-off has to be found between the electrical properties (which degrade with the Rh rate) and the high-temperature stability of the films (which improves with the Rh rate).

Acknowledgments

References

[1] J. Hornsteiner, E. Born, G. Fischerauer, and E. Riha, "Surface acoustic wave sensors for high temperature applications," in Proc. *IEEE Int. Freq. Contr. Symp.*, 1998, pp. 615–620.

[2] L . Reindl, C. C. W. Ruppel, A. Kirmayr, N. Stockhausen, and M. A. Hilhorst, "Passive radio requestable SAW water content sensor," in *Proc. IEEE Ultrasonics Symp.*, 1999, pp. 461–466.

[3] O. Elmazria, T. Aubert, "Wireless SAW sensor for high temperature applications: Material point of view," in Smart Sensors, Actuators, and MEMS V, SPIE Proceedings; SPIE: Bellingham, WA, USA, 2011; Volume 806602.

[4] M.P. Da Cunha, "Wireless Sensing in Hostile Environments," in *Proc. IEEE Ultrasonics Symp.*, 2013, pp. 1337-1346.

[5] T. Aubert, O. Elmazria, B. Assouar, L. Bouvot, M. Hehn, S. Weber, M. Oudich, D.Geneve, "Behavior of Platinum/Tantalum as interdigital transducers for SAW devices in high-temperature environments," *IEEE Trans. Ultrason. Ferroelectr. Freq. Control; Vol.* 58 (2011) 603–611.

[6] M. Pereira da Cunha, T. Moonlight, R. Lad, D. Frankel, G. Bernhardt, "High temperature sensing technology for applications up to 1000°C," *Proc. IEEE Sensors Symp.* (2008) 752–755.

[7] D.J. Frankel, S.C. Moulzolf, M.P. Da Cunha and R.J. Lad, "Influence of composition and multilayer architecture on electrical conductivity of high temperature Pt-alloy films," *Surface and Coatings Technology*, Vol. 284, pp. 215-221, 2015.

[8] M. Seifert, G.K. Rane, S. Oswald, S.B. Menzel and T. Gemming, "The Influence of the Composition of $Ru_{100-x}Al_x$ (x = 50, 55, 60, 67) Thin Films on Their Thermal Stability", *Materials* **2017**, *10*(3), 277.

[9] T. Aubert, J. Bardong, O. Legrani, O. Elmazria, B. Assouar, G. Bruckner and A. Talbi, "In situ high-temperature characterization of AlN-based surface acoustic wave devices", *Journal of Applied Physics*, 114, 014505, 2013.

[10] M. Lisker, T. Hur'yeva, Y. Ritterhaus and E.P. Burte, "Effect of annealing in oxygen atmosphere on morphological and electrical properties of iridium and ruthenium thin films prepared by liquid delivery MOCVD," *Surf. Coat. Tech.*, vol. 201, no. 22–23, 2007, pp. 9294–9298.

[11] D. Richter, S. Sakharov, E. Forsén, E. Mayer, L. Reindl, H. Fritze, "Thin Film Electrodes for High Temperature Surface Acoustic Wave Devices," *Procedia Engineering*, 25 ,2011, pp. 168–171.

[12] H. Osamura, N. Abe, "Development of new iridium alloy for spark plug electrodes, " *SAE Trans*. 108 (3) (1999) 1063–1074.

[13] A. Taguett, T. Aubert, M. Lomello, O. Legrani, O. Elmazria, J. Ghanbaja, A. Talbi, "Ir-Rh thin films as high-temperature electrodes for surface acousticwave sensor applications," *Sensors and Actuators A* 243 (2016) 35–42.

[14] T. Aubert, O. Elmazria, "Stability of langasite regarding SAW applications above 800°C in air atmosphere," in *Proc. IEEE Ultrasonics Symp.*, 2012, 2098–2101.

[15] P. Nicolay, T. Aubert, "A numerical method to derive accurate temperature coefficients of material constants from high-temperature SAW measurements: application to Langasite," *IEEE Trans. Ultrason. Ferroelectr. Freq. Control* 60 (October (10)) (2013) 2137–2141.

[16] Z.B. Bao, H. Murakami, Y. Yamabe-Mitarai, "Effects of thermal exposure on Ir-based alloys with and without Pt coating," *Corros. Sci*. 53 (2011) 1224–1229.